Conference Paper, Published Version

Van Ballegooy, S.; Meville, B. W.; Coleman, S. E.

Riprap and Cable-tied Block Performance as Scour Protection for Wing-wall Abutments Under Live Bed Conditions

RIPRAP AND CABLE-TIED BLOCK PERFORMANCE AS SCOUR PROTECTION FOR WING-WALL ABUTMENTS UNDER LIVE BED CONDITIONS*

VAN BALLEGOOY, S., MEVILLE, B.W., COLEMAN, S.E.
Civil and Environmental Engineering, The University of Auckland
Private Bag, Auckland, New Zealand

An experimental study of scour countermeasures for wing-wall abutments under live bed conditions is reported. The purpose of the study was to determine the required apron size to protect a wing-wall abutment from scour under live bed conditions, for different flow depths, flow velocities, and apron burial depths. Apron widths for both riprap and cable-tied block countermeasures were varied in size. It was observed that the troughs of the bed-forms that pass by the abutment undermine the apron, causing the outer edge of the apron to settle.

The results show that as the flow depth and flow velocity are increased, the outer edge of the apron settles into the sand, to a depth proportional to the height of the bed-forms developed in the flume. When the apron width is increased, the depth to which the outer edge settles remains constant. When the apron is pre-buried below the average bed level, the settlement of the outer edge is less, but the depth of the outer edge of the apron below the average bed level is the same as for the corresponding apron placed on top of the bed. The results also show that riprap and cable-tied block aprons respond in different ways. Stones on riprap aprons at the outer edge tend to settle and translate away from the abutment, pushing the bed-form troughs further away from the abutment. Conversely, because cable-tied block mats remain attached to the abutment, settlement of the apron allows the troughs of the bed-forms to pass closer to the abutment face.

From the study it is concluded that the scour at abutments under live bed conditions is governed by the size of the bed formations that pass the abutment. Therefore, the design of armoured scour countermeasures for abutments under live bed conditions should be based upon the largest expected bed formations. This will enable the settlement of the outer edge of the apron to be determined, and the required apron width to be chosen, depending on the tolerable distance between the troughs and the abutment.

1 Introduction

Scour countermeasures are used to protect bridge foundations from scour, mainly by inhibiting scour development at bridge piers and abutments. Rock riprap is the most common type of scour protection used at bridge abutments and approach embankments. Despite the widespread use of rock riprap, the guidelines for its use are based on limited research. Numerous alternative scour countermeasures now exist; one of the more recent developments being cable-tied blocks. Cable-tied blocks (CTB) comprise concrete blocks interconnected by stainless steel cable, giving a flexible concrete mattress. As a scour countermeasure, they have the advantage of ease of construction, minimal

* This work is supported by the US National Cooperative Highway Research Programme.

encroachment into the river channel, and a lower tonnage than riprap per unit area covered.

2 Present Study

A series of experiments was conducted in a 1.5-m-wide flume, to measure the equilibrium scour formation under live bed conditions at wing-wall abutments with riprap and cable-tied block aprons in place. The experimental set-up is shown in Figure 1a. The extent of protection, W and apron burial depth, b_d, were systematically varied. The scour formation varied according to the type and extent of protection around the abutment.

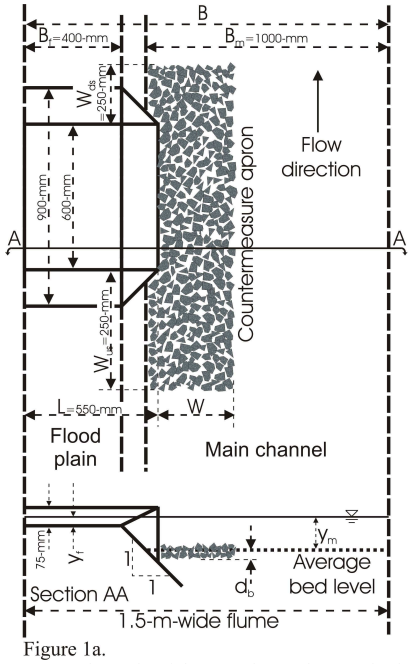

Figure 1a.

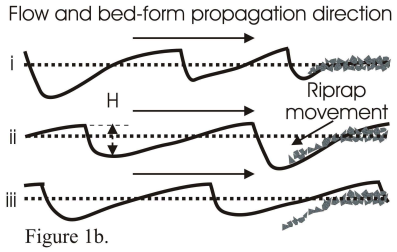

Figure 1b.

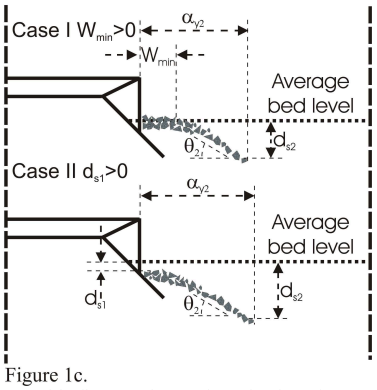

Figure 1c.

Figure 1a. Schematic of the experimental set-up in the 1.5-m-wide flume. Figure 1b. Behavior of an apron interacting with passing bed formations. Figure 1c. Equilibrium apron position

Two different flow depths were used, y_m=100-mm (bank-full) and y_m=170-mm (max flood level without overtopping the embankment), and four different flow velocities were used at each flow depth. Each flow condition was measured in the test section of the compound channel using a particle tracking velocimetry technique. The velocity was measured when the bed-forms in the main channel were fully developed. In order to generate appropriate flow velocities on the flood plain, it was necessary to increase the roughness. Rows of five evenly spaced 35x35x30-mm roughness blocks were glued onto the flood plain with a row spacing of 400-mm along the entire flood plain. For the bank-full condition the (main-channel) velocities tested were V/V_c=1.1, 1.4, 1.8 and 2.2. For the max flood level condition the velocities tested were V/V_c=1.1,1.5, 1.8 and 2.1.

The compound channel comprised a moveable-bed main channel, and a fixed flood channel. The sand used in the main channel had specific gravity of 2.65, median diameter d_{50}=0.82-mm and σ_g=1.3. A filter fabric with a pore space of 0.2-mm was placed beneath the apron. Riprap stones (with specific gravity of 2.65, D_{50}=40-mm and σ_g=1.1), were carefully placed to a thickness of $2D_{50}$ (equivalent to two riprap layers). The riprap aprons were tested at three different burial depths, $d_b=2D_{50}$ (80-mm), with the top of the apron flush with the average bed level, $d_b=1D_{50}$ (40-mm) and d_b=0, for which both layers were placed on top of the average bed-level. The cable-tied blocks had the shape of a square truncated pyramid with base dimensions 25x25-mm, height 10-mm and density 2084-kg/m^3. The blocks were glued onto shade cloth matting with pore spacing of 5-mm (to simulate the blocks being tied together with cables), with a 1-mm spacing around each block. The cable-tied mats were placed on the surface of the average bed level and attached to the abutment face. The mats were not tested at other burial depths. For the experiments at higher velocities, larger blocks were glued to the leading edge of the cable-tied block mat to prevent the mat from uplift (which causes the mat to overturn in the flow).

The heights of about 500 bed-forms (Figure 1b) were measured for most of the flow conditions using an echo sounder that traversed along the centreline of the main channel in the flume. The 95th percentile bed-form height, H_{95}, is given for each flow condition in Table 1.

Typical experimental setups are shown in Figure 2, for cable-tied block and riprap protection. Each run commenced from a flat bed. The flume slope was set to attain uniform flow conditions. Experimental durations ranged from 72-hours to 8-hours, being determined by an imposed requirement that at least 50 bed-forms would propagate past the abutment during the run.

Figure 2. Experimental set-up of a 0.3-m-wide apron placed around the abutment. Left; CTB apron placed on the surface. Right; riprap apron placed on top of the average bed level.

At the conclusion of each experiment, any sand covering the apron was carefully removed so that the settlement of the apron could be measured. The depth to which the outer edge of the apron had settled was taken as the maximum scour depth at that point. For each experiment, the settlement at the abutment face, d_{s1}, the settlement of the outer edge of the apron, d_{s2}, the horizontal distance from the abutment face to the outer edge of the apron, α_{y1} and the horizontal distance to the point where the apron was undermined, W_{min} were measured at both the upstream and downstream corners of the abutment

(Figure 1c and Table 1). Knowledge of d_{s1}, d_{s2}, W_{min} and α_{y2} allows investigation of the integrity of the wing-wall abutment, on the basis of a geotechnical slope stability analysis.

Table 1. Apron settlement parameters (in metres).

y_m	V/V_c	H_{95}	W	d_b	Upstream				Downstream			
					d_{s1}	d_{s2}	W_{min}	α_{y2}	d_{s1}	d_{s2}	W_{min}	α_{y2}
Cable-tied block apron												
0.10	1.1	0.083	0.1	0.00	-0.005	0.065	-	0.071	-0.005	0.060	-	0.076
0.10	1.4	0.080	0.1	0.00	0.020	0.090	-	0.071	0.015	0.080	-	0.076
0.10	1.8	0.081	0.1	0.00	-	-	-	-	-	-	-	-
0.10	2.2	-	0.1	0.00	-	-	-	-	-	-	-	-
0.17	1.1	0.097	0.1	0.00	0.075	0.145	-	0.071	0.065	0.135	-	0.071
0.17	1.5	0.105	0.1	0.00	-	-	-	-	-	-	-	-
0.17	1.8	0.122	0.1	0.00	-	-	-	-	-	-	-	-
0.17	2.1	0.136	0.1	0.00	-	-	-	-	-	-	-	-
0.10	1.1	0.083	0.2	0.00	-0.005	0.070	0.100	0.171	-0.005	0.065	0.100	0.176
0.10	1.4	0.080	0.2	0.00	-0.005	0.080	0.100	0.160	-0.005	0.070	0.075	0.179
0.10	1.8	0.081	0.2	0.00	0.000	0.110	0.025	0.161	-0.005	0.085	0.075	0.167
0.10	2.2	-	0.2	0.00	0.015	0.085	-	0.187	-0.005	0.085	0.075	0.167
0.17	1.1	0.097	0.2	0.00	-0.005	0.105	0.050	0.157	-0.005	0.075	0.075	0.175
0.17	1.5	0.105	0.2	0.00	0.005	0.135	0.025	0.136	0.000	0.125	0.025	0.147
0.17	1.8	0.122	0.2	0.00	0.000	0.135	0.025	0.136	-0.005	0.075	0.075	0.175
0.17	2.1	0.136	0.2	0.00	over turned				-0.005	0.160	0.000	0.120
0.10	1.1	0.083	0.3	0.00	-0.005	0.070	0.200	0.271	-0.005	0.065	0.200	0.276
0.10	1.4	0.080	0.3	0.00	-0.005	0.070	0.200	0.271	-0.005	0.070	0.175	0.279
0.10	1.8	0.081	0.3	0.00	-0.005	0.110	0.150	0.252	-0.005	0.095	0.150	0.266
0.10	2.2	-	0.3	0.00	0.010	0.155	0.100	0.226	-0.005	0.100	0.150	0.262
0.17	1.1	0.097	0.3	0.00	-0.005	0.070	0.175	0.279	-0.005	0.055	0.225	0.276
0.17	1.5	0.105	0.3	0.00	-0.005	0.125	0.100	0.256	-0.005	0.075	0.150	0.280
0.17	1.8	0.122	0.3	0.00	0.005	0.130	0.125	0.242	-0.005	0.090	0.175	0.262
0.17	2.1	0.136	0.3	0.00	0.035	0.185	-	0.260	-0.005	0.140	0.100	0.243
0.10	1.1	0.083	0.4	0.00	-0.005	0.070	0.300	0.371	-0.005	0.065	0.300	0.376
0.10	1.4	0.080	0.4	0.00	-0.005	0.075	0.300	0.366	-0.005	0.070	0.300	0.371
0.10	1.8	0.081	0.4	0.00	-0.005	0.115	0.225	0.357	-0.005	0.080	0.275	0.371
0.10	2.2	-	0.4	0.00	0.005	0.150	0.200	0.332	-0.010	0.130	0.200	0.352
0.17	1.1	0.097	0.4	0.00	-0.005	0.065	0.300	0.376	-0.005	0.055	0.300	0.384
0.17	1.5	0.105	0.4	0.00	-0.005	0.090	0.250	0.370	-0.005	0.065	0.300	0.376
0.17	1.8	0.122	0.4	0.00	-0.005	0.135	0.200	0.348	-0.005	0.085	0.275	0.367
0.17	2.1	0.136	0.4	0.00	-0.005	0.195	-	0.346	-0.010	0.130	0.250	0.325
Riprap apron												
0.10	1.1	0.083	0.1	0.08	0.000	0.080	0.050	0.200	0.000	0.060	0.070	0.165
0.10	1.4	0.080	0.1	0.08	0.005	0.085	0.000	0.200	0.000	0.065	0.070	0.165
0.10	1.8	0.081	0.1	0.08	0.010	0.095	-	0.230	0.000	0.075	0.050	0.200
0.10	2.2	-	0.1	0.08	0.040	0.110	-	0.240	0.000	0.105	0.000	0.240
0.17	1.1	0.097	0.1	0.08	0.000	0.105	0.040	0.300	0.000	0.085	0.060	0.250
0.17	1.5	0.105	0.1	0.08	0.000	0.105	0.000	0.230	0.000	0.085	0.060	0.230
0.17	1.8	0.122	0.1	0.08	0.000	0.135	0.000	0.260	0.000	0.105	0.040	0.250
0.17	2.1	0.136	0.1	0.08	0.105	0.175	-	0.325	0.000	0.145	0.040	0.305
0.10	1.1	0.083	0.2	0.08	0.000	0.075	0.100	0.300	0.000	0.055	0.150	0.270
0.10	1.4	0.080	0.2	0.08	0.000	0.085	0.080	0.310	0.000	0.055	0.150	0.280
0.10	1.8	0.081	0.2	0.08	0.000	0.120	0.060	0.320	0.000	0.065	0.150	0.300

0.10	2.2	-	0.2	0.08	0.000	0.125	0.040	0.340	0.000	0.085	0.150	0.300
0.17	1.1	0.097	0.2	0.08	0.000	0.103	0.100	0.300	0.000	0.100	0.130	0.320
0.17	1.5	0.105	0.2	0.08	0.000	0.130	0.080	0.350	0.000	0.100	0.130	0.320
0.17	1.8	0.122	0.2	0.08	0.000	0.140	0.060	0.360	0.000	0.095	0.130	0.345
0.17	2.1	0.136	0.2	0.08	0.025	0.145	-	0.360	0.000	0.115	0.100	0.360
0.10	1.1	0.083	0.3	0.08	0.000	0.085	0.200	0.380	0.000	0.045	0.250	0.360
0.10	1.4	0.080	0.3	0.08	0.000	0.085	0.200	0.390	0.000	0.065	0.250	0.370
0.10	1.8	0.081	0.3	0.08	0.000	0.095	0.180	0.415	0.000	0.065	0.230	0.380
0.10	2.2	-	0.3	0.08	0.030	0.120	0.150	0.470	0.000	0.075	0.220	0.410
0.17	1.1	0.097	0.3	0.08	0.000	0.085	0.200	0.400	0.000	0.075	0.230	0.390
0.17	1.5	0.105	0.3	0.08	0.000	0.105	0.180	0.405	0.000	0.075	0.230	0.380
0.17	1.8	0.122	0.3	0.08	0.000	0.110	0.150	0.410	0.000	0.105	0.200	0.390
0.17	2.1	0.136	0.3	0.08	0.000	0.165	0.100	0.470	0.000	0.115	0.150	0.390
0.17	1.1	0.097	0.1	0.04	0.005	0.13	-	0.3	-0.035	0.115	0.04	0.28
0.17	1.5	0.105	0.1	0.04	0.02	0.135	-	0.305	-0.035	0.115	0.04	0.285
0.17	1.8	0.122	0.1	0.04	0.07	0.16	-	0.305	0.005	0.115	-	0.285
0.17	2.1	0.136	0.1	0.04	-	0.19	-	0.35	0.025	0.165	-	0.36
0.17	1.1	0.097	0.2	0.04	-0.035	0.12	0.09	0.385	-0.035	0.09	0.1	0.355
0.17	1.5	0.105	0.2	0.04	-0.035	0.125	0.05	0.385	-0.035	0.09	0.1	0.355
0.17	1.8	0.122	0.2	0.04	-0.035	0.13	0.05	0.36	-0.035	0.11	0.09	0.37
0.17	2.1	0.136	0.2	0.04	0.075	0.165	-	0.45	-0.035	0.165	0.05	0.43
0.17	1.1	0.097	0.3	0.04	-0.035	0.105	0.15	0.4	-0.035	0.075	0.2	0.4
0.17	1.5	0.105	0.3	0.04	-0.035	0.13	0.15	0.47	-0.035	0.12	0.2	0.46
0.17	1.8	0.122	0.3	0.04	-0.035	0.135	0.15	0.47	-0.035	0.13	0.2	0.46
0.17	2.1	0.136	0.3	0.04	0.045	0.165	-	0.53	-0.035	0.145	0.15	0.515
0.17	1.1	0.097	0.1	0.00	0.005	0.115	-	0.36	-0.075	0.095	0.04	0.35
0.17	1.5	0.105	0.1	0.00	0.045	0.145	-	0.36	-0.075	0.105	0.04	0.35
0.17	1.8	0.122	0.1	0.00	0.075	0.165	-	0.36	-0.005	0.145	-	0.43
0.17	2.1	0.136	0.1	0.00	-	-	-	-	-	-	-	-
0.17	1.1	0.097	0.2	0.00	-0.075	0.13	0.06	0.43	-0.075	0.12	0.09	0.42
0.17	1.5	0.105	0.2	0.00	-0.075	0.14	0.04	0.43	-0.075	0.125	0.09	0.43
0.17	1.8	0.122	0.2	0.00	-0.025	0.14	-	0.44	-0.075	0.125	0.06	0.44
0.17	2.1	0.136	0.2	0.00	0.035	0.155	-	0.45	-0.075	0.145	0	0.46
0.17	1.1	0.097	0.3	0.00	-0.075	0.115	0.15	0.49	-0.075	0.095	0.2	0.47
0.17	1.5	0.105	0.3	0.00	-0.075	0.125	0.15	0.49	-0.075	0.1	0.2	0.48
0.17	1.8	0.122	0.3	0.00	-0.075	0.135	0.09	0.51	-0.075	0.115	0.15	0.49
0.17	2.1	0.136	0.3	0.00	0.045	0.145	-	0.51	-0.075	0.135	0.15	0.53

3 Results

As the bed-forms propagated past the apron, the troughs of the bed-forms were observed to undermine the outer edge of the apron, as shown in Figure 1bi. In the case of a riprap apron, the riprap at the outer edges tended to move forward and down into the bottom of the troughs, whereas a cable-tied block apron was constrained to settle in the downward direction only. This settling process continued as subsequent bed-forms with deeper troughs passed the apron, further undermining the toe of the apron (Figure 1bii). Subsequent bed-forms, with shallower troughs, propagated over the apron without causing further settlement (Figure 1biii). After a sufficient number of bed-forms had passed, the edge of the apron was assumed to have settled to its equilibrium position.

Increased flow depth and flow velocity increased the scour depth at the outer edge of the apron considerably. Increasing the burial depth of the apron did not affect the scour

depth at the outer edge of the apron, although the apron remained more intact at the end of the experiment, i.e. W_{min} increased with increasing burial depth because less material was undermined from the apron. Increasing the apron width had little effect on the scour depth at the outer edge of the apron.

Conversely, experimental work under clear-water conditions (van Ballegooy et al, 2004) clearly shows that the local scour depth reduces with increased apron width, because the local scour hole is deflected further from the abutment. Similar trends would also be expected for live-bed conditions. The maximum equilibrium scour depth as a function of the mean flow velocity occurs at threshold conditions and decreases slightly thereafter with increasing velocity (Breusers and Raudkivi, 1991). Two initial experiments were run just below threshold conditions for 72-hrs without any protection to determine the maximum local scour depth at the abutment for the two flow depths used. For both experiments the deepest point of scour occurred at the upstream corner of the abutment face, with a maximum scour depth, d_s, of 90-mm for the 100-mm flow depth and 105-mm for the 170-mm flow depth. Repeating the experiments with a 200mm-wide apron significantly reduced the maximum scour depth. These measured local scour depths for clear-water conditions are considerably smaller than the measured scour depths at the outer edge of the apron for live-bed conditions, which is contrary to what would be expected. It is apparent that the troughs of the bed-forms in the live-bed experimental work were very much deeper than the local scour at the abutment, the former therefore dominating the maximum scour depth d_{s2}.

The exeriments showed that the protection apron typically settles to the level of the deepest bed-form trough that propagates past the abutment during the particular runs. At the upstream corner of the abutment the scour depth d_{s2} was taken equal to the maximum trough depth. At the downstream corner of the abutment d_{s2} was taken equal to 80% of the maximum trough depth.

The upstream scour depth is larger than the downstream scour depth, because the bed-forms tend to reduce in size as they propagate past the abutment. At the downstream end of the abutment, the flow is fully contracted in the main channel. Consequently, the velocity increases which causes the crests of the bed-forms to wash out and the troughs to fill in. Because the troughs of the bed-forms control d_{s2}, both riprap and cable-tied block mat aprons have the same settlements of the outer edge of the apron.

The angle θ_2 (defined in Figure 1c), can be simply obtained from d_{s1}, d_{s2}, W_{min} and α_{y2}. θ_2 was found to be invariably 25° for the riprap aprons and 50° for the cable-tied block aprons at both the upstream and downstream corners of the abutment. The difference of the two angles can be directly related to the behaviour of the different apron types. Because the cables prevent the block aprons from increasing in width, sand is eroded from beneath the apron and the outer edge of the apron folds down retaining the sand at an angle larger than the repose angle of the sand. When a riprap apron is undermined, the apron increases in width as the riprap stones roll forward and down into the bottom of the troughs, and the stones stabilise at an angle slightly less than the repose angle of the sand.

For Case I (Figure 1c where $W_{min} > 0$) W_{min} was found to increase linearly with increasing apron width. From the data it can also be seen that W_{min} increases with apron burial depth and decreases with increasing flow depth and velocity. Considering Figure 3a, because cable-tied block aprons cannot extend in width, the sum of W_{min} and the

sloping portion of the mat must be equal to W. Considering Figure 3b, because the riprap apron comprises of two layers, it can be assumed that the sum of W_{min} and one half of the sloping portion of the apron is equal to W. In this way a simple model can be developed to predict W_{min} (Equation 1), as follows

$$W_{min} = W - \frac{b}{\sin\theta_2}(d_s - d_b) \quad (1)$$

where b = 1 for cable-tied block aprons, b = c/η for riprap aprons, c = coefficient depending on location and η = the number of riprap layers. At the downstream corner of the abutment c = 1, because the riprap translates laterally as erosion occurs. At the upstream corner of the abutment, $c = \sqrt{2}$, because the troughs of the bed-forms undermine the upstream edge and the side of the apron. This causes the riprap stones move both laterally and longitudinally.

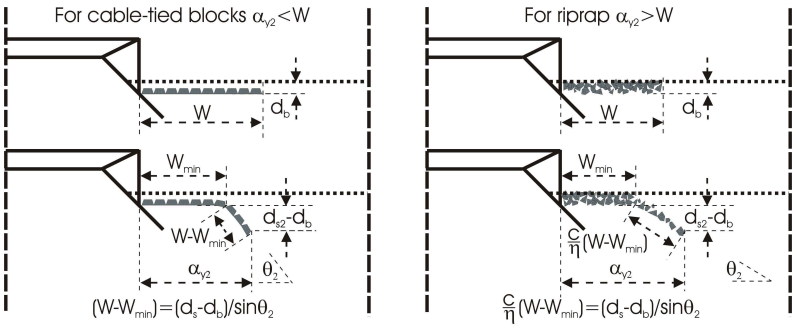

Figure 3a. Figure 3b.

Figure 3a. Mode of settlement of a cable-tied block apron. Figure 3b. Mode of settlement of a riprap apron.

Equation 1 shows that W_{min} increases linearly with W, which is in agreement with the experimental data. W_{min} decreases with increasing d_{s2}, reflective of deeper flow depths and higher flow velocities. W_{min} also increases with increasing d_b. The deeper the apron is buried below the average bed level, the smaller the volume of the material undermined from the apron. When the apron is buried below the expected scour depth ($d_b > d_s$), the apron cannot be undermined, so there is no apron loss ($W = W_{min}$). The value of the coefficient ($b/\sin\theta_2$) for the different apron types shows that W_{min} is significantly larger for cable-tied block aprons compared to equivalent riprap aprons at the upstream corner of the abutment. However, at the downstream corner of the abutment W_{min} is approximately the same for both cable-tied block and riprap aprons. The former observation is because the riprap stones have a two-directional movement at the upstream edge of the apron when it is undermined, whereas the cable-tied blocks cannot move but only settle. For $W_{min} > 0$, it can be concluded that cable-tied block aprons provide greater protection from scour at the abutment in terms of the parameter W_{min}, than for equivalent riprap aprons, provided that the upstream leading edge of the cable-tied block apron does not lift due to the hydrodynamic forces exerted on the mat by the flow.

When $W_{min} > 0$, an expression for α_{y2} can be simply developed from Figure 1c as follows

$$\alpha_{y2} = W_{min} + \frac{d_s - d_b}{\tan \theta_2} \quad (2)$$

From Equation 2 it can be seen that α_{y2} exceeds W for settled riprap aprons, because the stones from the riprap apron tend to settle and translate away from the abutment face, pushing the troughs of the bed-forms further away from the abutment. Conversely α_{y2} is less than W for settled cable-tied block aprons, allowing the troughs of the bed-forms to pass closer to the abutment face (Figure 3).

For Case II (Figure 1c where $d_{s1} > 0$), insufficient protection has been placed around the abutment ($W_{min} < 0$). In this case cable-tied block aprons offer little protection at all, and in most cases act to increase the scour depth at the abutment face. This is because the apron is attached to the abutment face and becomes an obstruction in the flow at the abutment face. Conversely, when an insufficient riprap apron is placed around the abutment, the apron settles at the abutment face (i.e. $d_{s1} > 0$), but still offers some protection at the abutment face, because the scour depth at the abutment face, d_{s1} is still less than d_{s2}.

4 Application

Equations 1 and 2 are the basis of a method for assessment of the integrity of wing-wall bridge abutments. The method enables determination of the local equilibrium scour formation for an abutment, for a given level and type of scour countermeasure protection. A geotechnical slope-stability analysis can be undertaken on an axis perpendicular to the abutment face to assess the structural integrity of the abutment. This method has the advantage that the countermeasure protection can be designed to be site specific for each bridge abutment. Abutments with deep foundations may not require much countermeasure protection, because larger scour hole formations closer to the abutment may be tolerable. Conversely, for abutments with shallow foundations, the designer may require more countermeasure protection, because scour formations in close proximity to the abutment would compromise the structural integrity of the bridge. If the level of protection provided predicts an undesirable scour formation at the abutment, the designer can increase the level of protection provided or change the type of protection provided, until the expected scour at the abutment is tolerable.

5 Conclusions

The conclusions from this experimental study are:

- For the range of experimental investigation in this study, the scour at wing-wall abutments in live-bed conditions is directly related to the level of the deepest bed-form trough that propagates past the abutment.

- Stones on the outer edge of riprap aprons tend to settle and move away from the abutment pushing the troughs of the bed-forms further away from the abutment. Conversely, cable-tied block mats remain intact during settlement. The outer edge of the apron settles vertically, allowing the troughs of the bed-forms to pass closer to the abutment face than for an equivalent riprap apron.
- Equation 1 allows prediction of the minimum apron width remaining horizontal after erosion. Equation 2 allows prediction of the horizontal distance between the abutment face and the point of deepest scour. These predictions facilitate assessment of the stability of an abutment structure.

References

Breusers, H.N.C. and Raudkivi, A.J. (1991) “Scouring”, Hydraulic Structures Design Manual, No. 2, I.A.H.R., Balkema, Rotterdam, Netherlands.

van Ballegooy, S. Melville, B.W. and Coleman, S.E. (2004). "Riprap And Cable-tied Block Protection for Spill-through Abutments", Proceedings of the 2nd International Conference on Scour and Erosion, ICSE-2, Singapore, Nov. 14-17.